Int J Clin Exp Pathol 2015;8(4):3727-3734
www.ijcep.com /ISSN:1936-2625/IJCEP0006291

Original Article

Spatiotemporal expression of BMP7 in the development of anorectal malformations in fetal rats

Jin Zhang[1], Xiao-Bing Tang[1], Wei-Lin Wang[1], Zheng-Wei Yuan[2], Yu-Zuo Bai[1]

[1]*Department of Pediatric Surgery, Shengjing Hospital, China Medical University, Shenyang 110004, PR China;*
[2]*The Key Laboratory of Health Ministry for Congenital Malformation, Shenyang 110004, PR China*

Received January 23, 2015; Accepted March 22, 2015; Epub April 1, 2015; Published April 15, 2015

Abstract: The aim of this study was to determine the expression patterns of bone morphogenetic protein 7 (BMP7) during anorectal development in normal rat embryos and in embryos with anorectal malformations (ARM), and to investigate the possible role of BMP7 in the pathogenesis of ARM. ARM was induced by treating rat embryos with ethylenethiourea on the 10th gestational day (GD10). Embryos were harvested by Cesarean delivery and the spatiotemporal expression of BMP7 was evaluated in normal (n=168) and ARM embryos (n=171) from GD13 to GD16 using immunohistochemistry staining and western blot analysis. Immunohistochemical staining in normal embryos revealed that BMP7 was abundantly expressed on the epithelium of the urorectal septum (URS) and the hindgut on GD13, and BMP7-immunopositive cells were extensively detected in the URS, hindgut, and cloacal membrane by GD14. Increased positive tissue staining was noted on the fused tissue of the URS and the thin anal membrane on GD15. In ARM embryos, the epithelium of the cloaca, URS, and anorectum were negatively or only faintly immunostained for BMP7. BMP7 protein expression showed time-dependent changes in the developing hindgut according to western blotting, and reached a peak on GD15 during anus formation. BMP7 expression levels from GD14 to GD15 were significantly lower in the ARM group compared with the normal group ($P<0.05$). Spatiotemporal expression of BMP7 was disrupted in ARM embryos during anorectal morphogenesis from GD13 to GD16. These results suggest that downregulation of BMP7 at the time of cloacal separation into the primitive rectum and UGS might be related to the development of ARM.

Keywords: Anorectal malformation, BMP7, embryogenesis, development, rat

Introduction

Anorectal malformations (ARM) are common surgical disorders affecting 1 in 5,000-1,500 live births [1]. Despite advances in the surgical and medical care of infants with ARM [2], their quality of life remains adversely affected [3-5]. However, ARM is a complex multigene disease and its etiology, embryology, and pathogenesis are poorly understood and controversial. It is therefore essential to develop a better understanding of the developmental basis of normal and abnormal anorectal organogenesis [6]. ARM might result from mutations in a variety of genes, and elucidation of the expression patterns of several genes during various stages of gastrulation have shed light on the molecular basis of this condition. Bone morphogenetic protein (BMP) signaling plays crucial roles in forming and patterning ventral and posterior tissues during vertebrate embryogenesis [7-9]. BMP7 is a member of the BMP family. BMP7 has been shown to be expressed in the urorectal mesenchyme (URM), and loss of BMP7 function results in the arrest of cloacal septation [10]. BMP7 expression was detected within several specific domains in the cloacal epithelium and mesenchyme during mid-gestation in mouse embryos, and was present in the urethra and rectum during late embryogenesis. BMP7 expression and the null phenotype indicate that BMP7 may play an important role in reorganization of the epithelium during cloacal septation and morphogenesis of the genital tubercle [11]. Although these previous studies suggest a relationship between BMP7 and anorectal morphogenesis, its expression patterns during the embryogenesis of ARM have not yet been investigated. We therefore analyzed the distribution of BMP7 protein in normal and eth-

Table 1. Distribution of embryos in the various age and treatment groups

Age group	Normal		ARMs	
	IHC	WB	IHC	WB
GD13	24	24	26	26
GD14	23	24	24	25
GD15	23	23	23	25
GD16	20	21	23	23
Total	90	92	96	99

Note: ARMs anorectal malformations, IHC immunohistochemical staining, WB Western blot, GD gestational day.

ylenethiourea (ETU)-induced-ARM rat embryos, with an emphasis on embryonic stages GD13 to GD16, which are the critical time-points in anorectal development.

Materials and methods

Animal model and tissue collection

Mature Wistar rats (body weight, 250-300 g) were provided by the Medical Animal Center, Shengjing Hospital of the China Medical University (Shenyang, PR China). Ethical approval was obtained from the China Medical University Animal Ethics Committee before the start of the study. The procedures for creating ARM in fetal rats have been described previously [12]. Fifty time-mated pregnant Wistar rats were randomly divided into two groups: an ETU-treated group and a control group. In the ETU-treated group, 30 pregnant rats were gavage-fed a single dose of 125 mg/kg of 1% ETU (2-imidazolidinethione; Aldrich Chemical, Penzberg, Germany) on GD10 (GD0=sperm in vaginal smear after overnight mating). Twenty control rats received corresponding doses of ETU-free saline on GD10. Embryos were harvested by Cesarean delivery on GD13 to GD16. About a third of the embryos were fixed in 4% paraformaldehyde for 12-24 hours, depending on their size. Embryos from each age group were then dehydrated and embedded in paraffin and serial sagittal sections were cut at 4-μm thickness for immunohistochemical staining (IHC). Embryos were subsequently divided into normal and ARM embryos based on the presence of ARM determined under a light microscope. Other specimens were frozen in liquid nitrogen and sequential sagittal sections were cut on a cryostat, mounted on coated glass slides, and examined under a microscope to confirm the occurrence of ARM in ETU-treated embryos. Embryos with or without ARM were thus distinguished by light microscopy prior to microdissection. The cloaca was dissected from GD13 to GD14 embryos, removed free from surrounding tissues under magnification, and immediately frozen in liquid nitrogen for western blot analysis. Full-thickness rectum was also dissected from GD15 and GD16 specimens. The equivalent regions of normal embryos were also microdissected. Embryos were therefore divided into normal and ARM groups, confirmed by light microscopy.

IHC staining

Endogenous peroxidase activity was blocked by incubation in 3% hydrogen peroxide for 20 min. Antigen retrieval was performed by heating the slides in 10 mM citrate buffer (pH 6.0) at 98°C for 8 min. The sections were treated and incubated with primary anti-BMP7 (1:200 rabbit polyclonal, Abcam, UK) and horseradish peroxidase (HRP)-conjugated secondary antibody (Santa Cruz Biotechnology, CA, USA). Antibody incubations were performed in phosphate-buffered saline supplemented with 10% goat serum. Primary antibody was incubated with the sections at 4°C for 16 h, and the secondary antibody was incubated for 20 min at room temperature. Signals were visualized using 3,3' diaminobenzidine (Sigma, UK). Sections were counterstained with hematoxylin. Negative controls were performed by either omitting the primary or secondary antibody or incubating with the equivalent concentrations of nonimmune rabbit antiserum. Two pathologists independently reviewed the IHC-stained slides and the results were agreed by consensus.

Protein preparation and western blot

Protein preparation was performed as described previously [13]: cloaca/hindgut were pooled and sonicated in distilled deionized water containing protease inhibitors. Protein extracts (50 μg) were heated at 100°C for 5 min and size fractionated by Bis-Tris sodium dodecyl sulfate-polyacrylamide gel electrophoresis (SDS-PAGE) (Invitrogen, Carlsbad, CA, USA). Protein samples were denatured, separated by SDS-PAGE, transferred to polyvinylidene fluoride membranes (Millipore, Billerica, MA, USA), blocked with 5% fat-free milk in Tris-buffered saline (2 h, room temperature), and

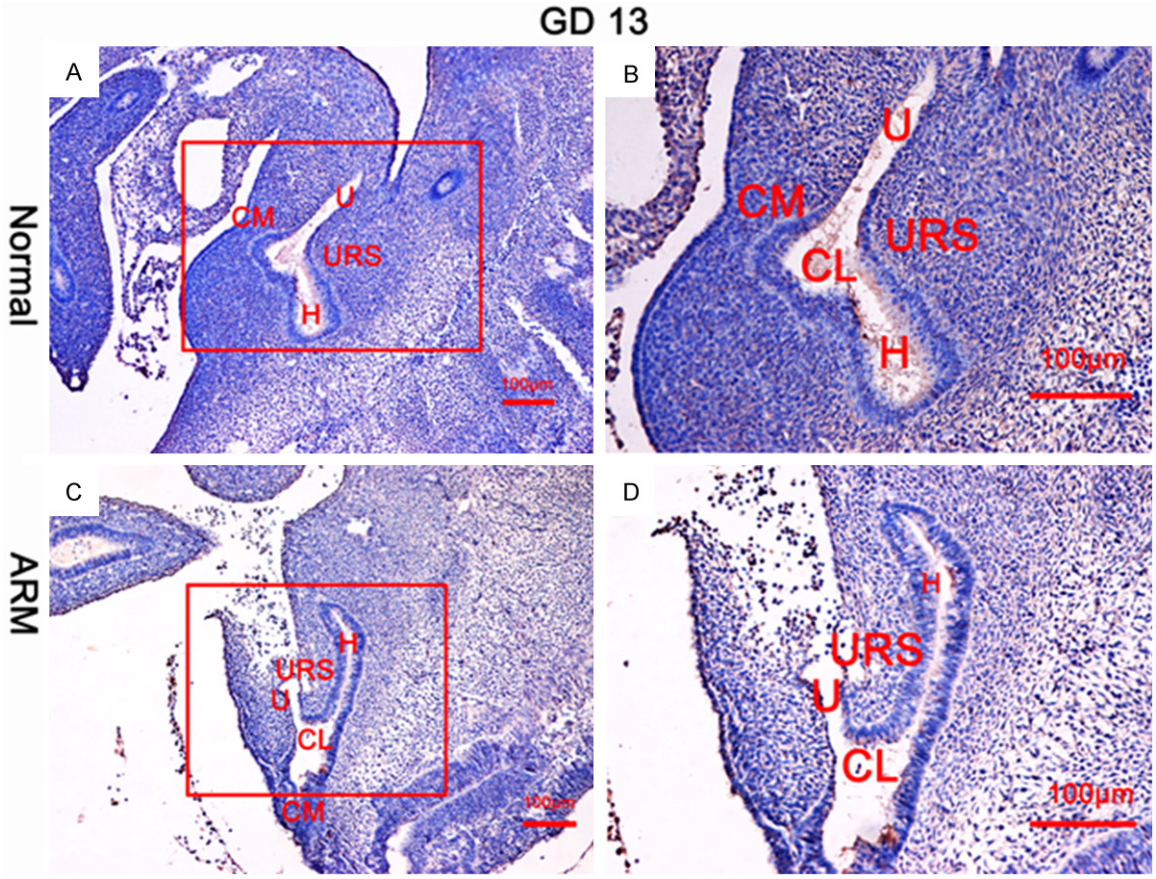

Figure 1. (A, B) Normal embryos. On GD13, BMP7-immunopositive cells were abundantly detected in the epithelium of the urorectal septum (URS) and hindgut (H). (C, D) Anorectal malformation (ARM) group. On GD13, sporadic BMP7-immunolabeled cells were detected on the URS and hindgut (U urethra, CL cloaca, CM cloacal membrane). Red rectangles in (A and C) are shown at higher magnification in (B and D) respectively. Original magnification: ×100 (A, C), ×200 (B, D).

incubated overnight at 4°C with primary antibody against BMP7 (diluted 1:500) and mouse monoclonal antibody to glyceraldehyde-3-phosphate dehydrogenase (GAPDH) (diluted 1:15000; Sigma, St Louis, MO, USA). Membranes were washed and incubated with secondary antibody (rabbit anti-goat or goat anti-mouse HRP conjugate; Jackson Immunoresearch, West Grove, PA, USA) for 2 h at room temperature. Following a further washing, membranes were developed using a chemiluminescent substrate kit (Pierce, Rockford, IL, USA). For western blot analysis, densitometric values were analyzed by using an ECL Plus detection system (Millipore).

Results

General observations

No malformations were observed in the 182 embryos from normal rats. However, all 241 ETU-treated embryos had short or no tail, and 15 of the embryos died *in utero*. The incidence of ARM in ETU-treated embryos was 80.9% (195/241). The embryos used for IHC and western blot in each group are shown in **Table 1**. The type of ARM was rectourethral fistula or persistent cloaca.

IHC results

Normal group: On GD13, the L-shaped URS divided the cloaca into the urogenital sinus ventrally and the primitive rectum dorsally. BMP7-immunopositive cells were abundantly detected in the epithelium of the URS and hindgut (**Figure 1A**, **1B**). On GD14, there was a potential canal between the tip of the URS and the cloacal membrane (CM), and BMP7-immunopositive cells were extensively detected in the URS, hindgut, and CM (**Figure 2A**, **2B**). On GD15, the epithelium on the tip of the URS fused with that

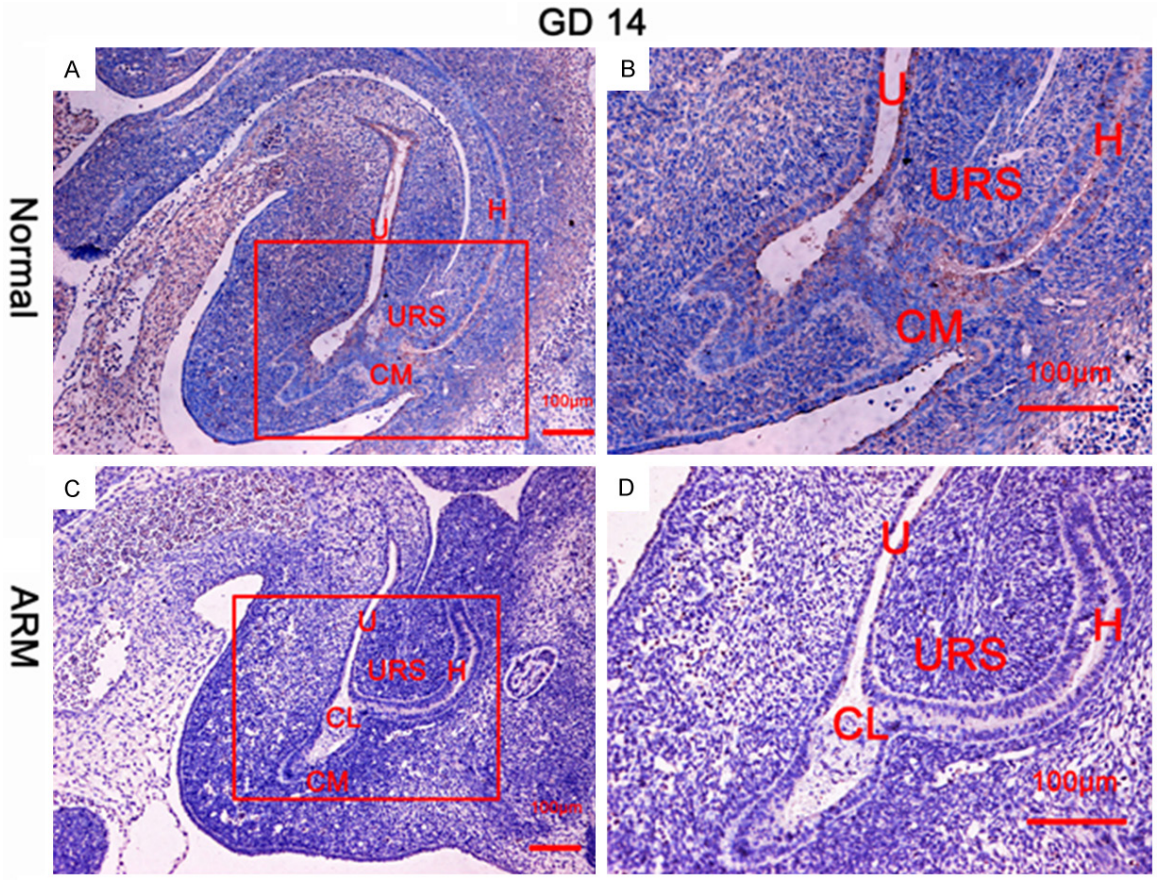

Figure 2. (A, B) Normal group. On GD14, BMP7-immunopositive cells were extensively detected on the urorectal septum (URS), hindgut (H), and cloacal membrane (CM). (C, D) ARM group. On GD14, BMP7 was faintly expressed on the epithelium of the URS and hindgut. (U urethra, CL cloaca). Red rectangles in a and c are shown at higher magnification in b and d, respectively. Original magnification: ×100 (A, C), ×200 (B, D).

of the dorsal CM leading to the separation of the hindgut and urogenital sinus (UGS). The anal membrane was almost ruptured. The fused tissue of the URS and the thin anal membrane were strongly and constantly immunopositive for BMP7 (**Figure 3A**, **3B**). On GD16, the rectum separated from the UGS completely, the anal membrane ruptured, and the anorectum communicated with the outside. BMP7-immunolabeled cells were observed on the anorectal epithelium (**Figure 4A**, **4B**).

ARM group: On GD13, the distance between the URS and the CM was relatively long, while the CM was shorter and thicker than normal. Sporadic BMP7-labeled cells were detected on the dorsal URS and hindgut (**Figure 1C**, **1D**). On GD14, the URS was high in the cloacal cavity, and the distance between the URS and the CM was still relatively long. BMP7 was faintly expressed on the epithelium of the URS and the hindgut (**Figure 2C**, **2D**). On GD15, the distance between the URS and cloacal membrane had decreased; however, the URS did not fuse with the CM, and a fistula was evident between the rectum and urethra. The hindgut did not separate from the UGS. BMP7-positive cells were sparsely located on the epithelium of the fistula, URS, and rectum (**Figure 3C**, **3D**). On GD16, the rectal terminus was not connected to the outside, and BMP7-immunolabeled cells were sparse on the epithelium of the fistula and anorectum (**Figure 4C**, **4D**).

Western blot analysis

Western blotting was performed to quantify BMP7 protein expression during the development of the cloaca/hindgut. BMP7 was detected as a band of about 49 kDa among the proteins extracted from both normal and ARM tissues. Each protein band was normalized to a

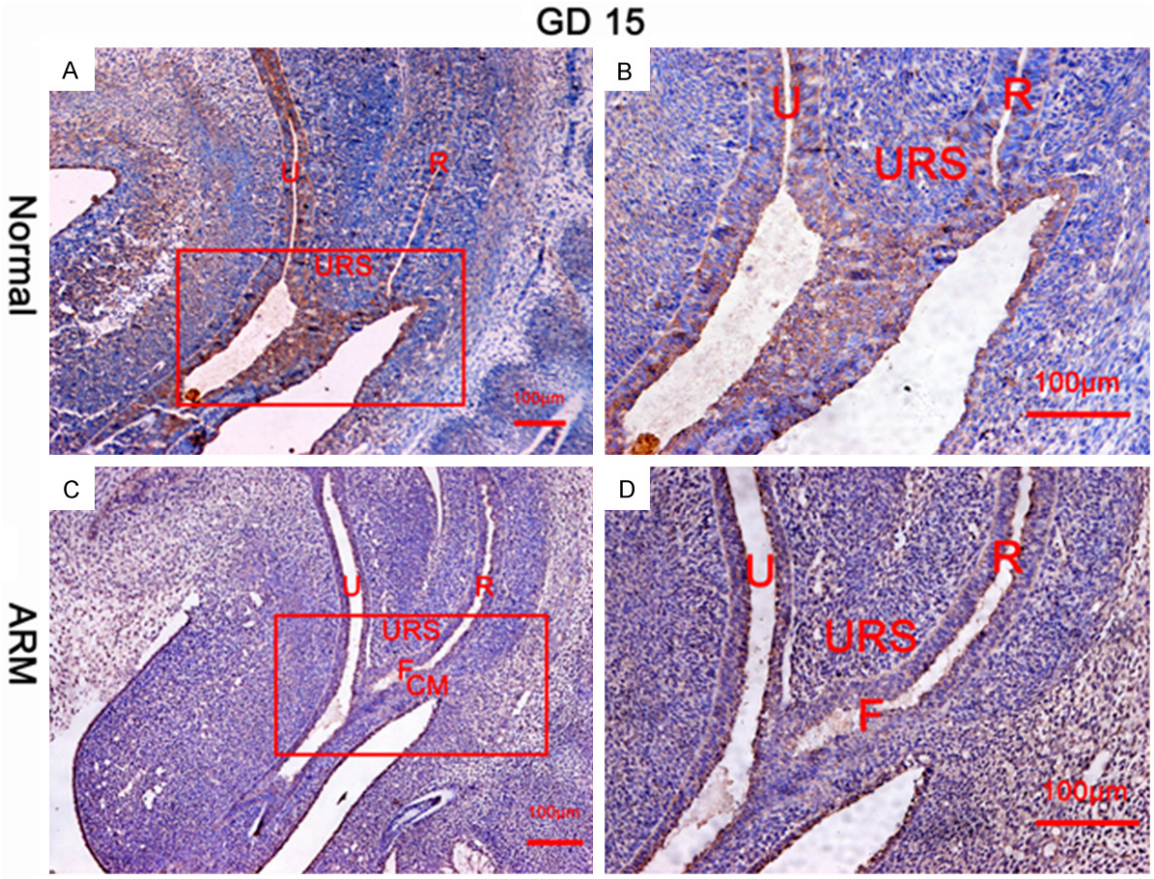

Figure 3. (A, B) Normal group. On GD15, the epithelium on the tip of the urorectal septum (URS) fused with that of the dorsal cloacal membrane (CM) leading to separation of the hindgut and urogenital sinus. The fused tissue of the URS and the thin anal membrane were constantly immunoreactive for BMP7 (R rectum). (C, D) ARM group. On GD15, the URS did not fuse with the CM, and a fistula (F) was evident between the rectum (R) and urethra (U), allowing the rectum and urethra to communicate with each other. BMP7-positive cells were sparsely located on the epithelium of the fistula, URS, and rectum. Red rectangles in (A and C) are shown at higher magnification in (B and D), respectively. Original magnification: ×100 (A, C), ×200 (B, D).

corresponding GAPDH band (**Figure 5**). BMP7 expression reached maximal levels in the normal group on GD14 and GD15, which are the key periods of anus formation, but remained relatively low in the ARM group. BMP7 protein expression was significantly decreased in the ARM hindgut compared with normal hindgut in each age group (GD13, 0.450±0.007 vs. 0.352±0.008; GD14, 0.796±0.006 vs. 0.334 ±0.007; GD15, 0.903±0.011 vs. 0.620±0.010; GD16, 0.755±0.006 vs. 0.656±0.002; $P<0.05$). BMP7 expression began to decrease on GD16 in the normal group when the URS divided the cloaca into the primitive rectum and UGS.

Discussion

Mice and rats provide suitable models for studying human embryonic development, and are a valuable tool for determining the molecular mechanisms involved in cloaca malformations [14]. In this study, we investigated the expression of BMP7 during the development of ARM in fetal rats. BMP7 signaling is one of the primary signal transduction pathways in embryogenesis. BMP7 is a member of the transforming growth factor-β superfamily of growth factors and a target gene of Sonic hedgehog [13]. BMP7 is a highly-pleiotropic growth factor [15]. Loss of BMP7 function results in the arrest of cloacal septation and defects in cell adhesion in the urethral endoderm [11], while signaling by BMP7 regulates polarity in cell division and cell-fate choice in the cloacal endoderm [10]. A previous study showed that disruption of epithelial hedgehog signaling resulted in alterations in BMP signal-

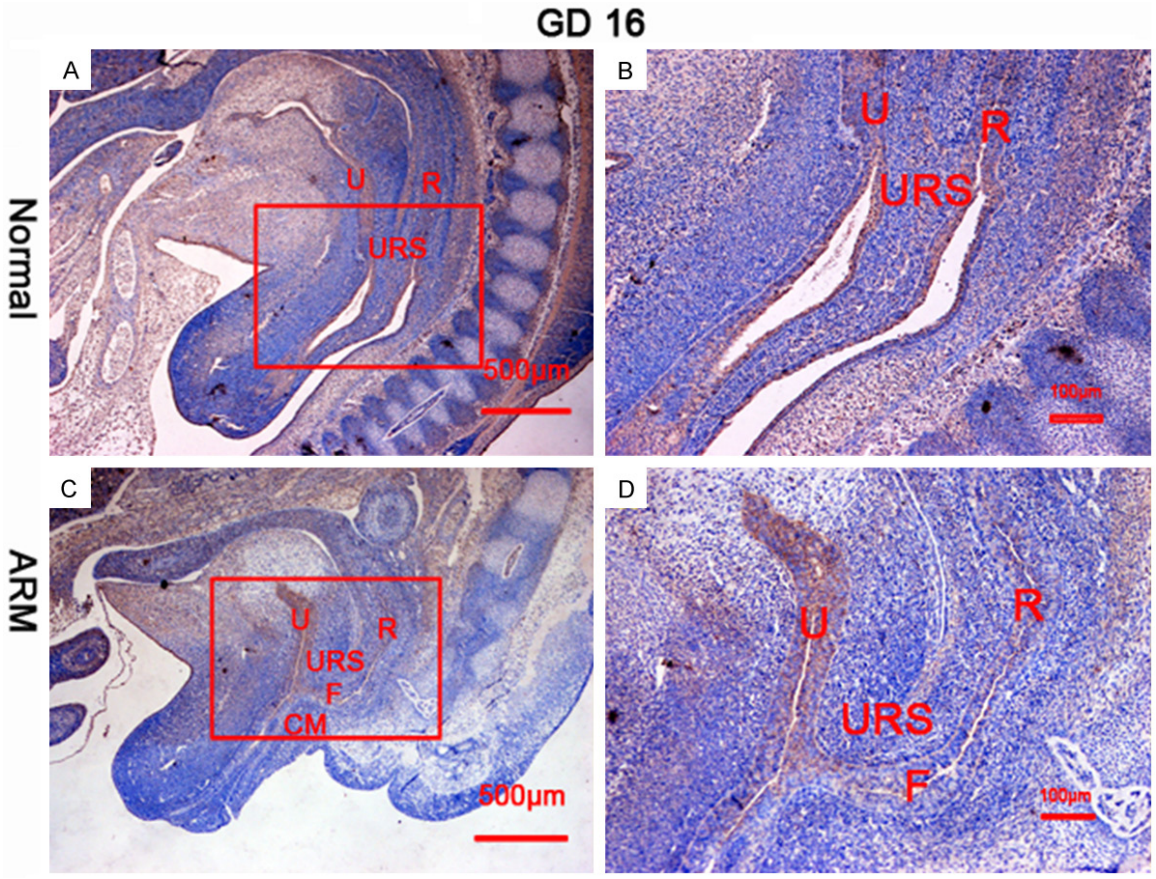

Figure 4. (A, B) Normal group. On GD16, BMP7-immunolabeled cells were observed on the anorectal epithelium (R rectum, U urethra, URS urorectal septum). (C, D) ARM group. On GD16, few BMP7-immunolabeled cells were detected on the epithelium of the fistula (F) and rectum (R). Red rectangles in (A and C) are shown at higher magnification in (B and D) respectively. Original magnification: ×40 (A, C), ×100 (B, D).

ing in the surrounding mesenchyme, causing early abnormal differentiation of the cloacal endoderm and subsequent hypervascularity in the stroma surrounding the cloaca [14]. It is therefore important to examine the important role of BMP7 during the normal development of the cloaca. ETU has previously been employed to study morphological changes in ARM in rat embryos [6, 12, 13, 16, 17]. In the current study, we investigated the spatial and temporal expression patterns of BMP7 during anorectal development by IHC and western blotting. In normal rat embryos, BMP7 expression peaked on GD14 and GD15, but decreased after anus formation. However, in ARM embryos, BMP7 expression levels remained low and unchanged, suggesting that BMP7 might play an essential role not only in the embryogenesis of the anorectum, but also in the development of ARM.

In this study, BMP expression in the anorectum showed different spatial distributions in normal and ARM embryos. From GD13 to GD15, BMP7-immunopositive cells were extensively detected in the key region during the progress of URS fusion with the CM. In contrast, only sporadic BMP7 immunostaining was evident in this region in ARM embryos. There were therefore spatial differences in BMP7 expression between normal and ARM embryos during embryogenesis of the anorectum. These results suggest that morphogenic events in the anorectum depend on BMP7 signal transduction, and that aberrations in BMP7 may be responsible for abnormal morphogenesis of the anorectum. Accordingly, the expression of BMP7 protein in abnormal regions might contribute to disturbances in proliferation/differentiation in the local microenvironment, inducing mistranscription of target genes and further maldevelopment of structures.

In addition, western blot analysis showed that BMP7 expression in normal embryos peaked

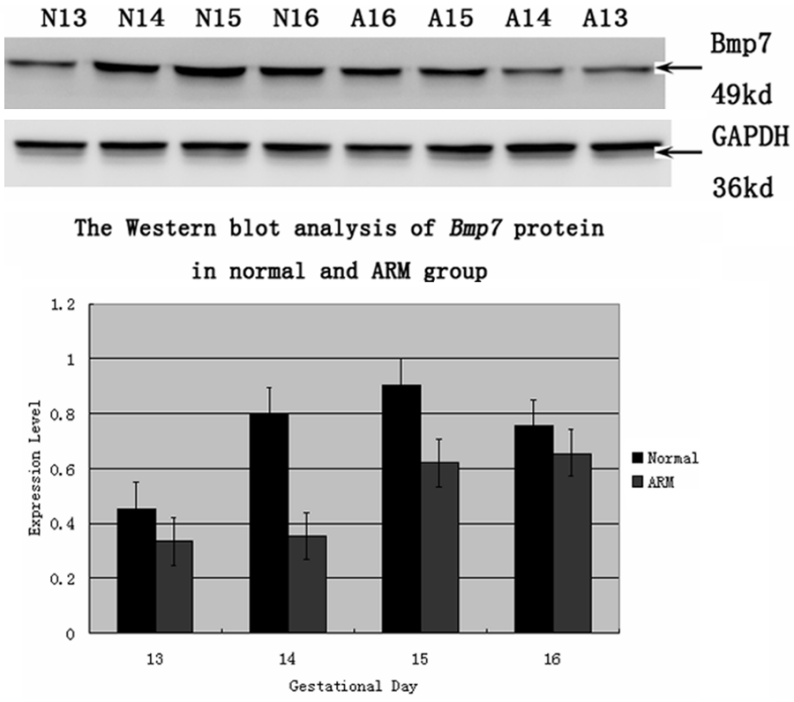

Figure 5. Western blot analysis of BMP7 protein expression levels in normal and ARM developing hindgut tissue samples. Values are presented as means ± standard deviation. Top, BMP7 was detected as an approximately 49-kDa band on western blots. Immunoblots showed a strong signal for BMP7 protein in the normal group, but a weak signal in the ARM group. GAPDH was used as an internal control. Bottom, histogram showing the trends of BMP7 expression at each time-point. A peak is evident on GD15.

during the critical period of anorectal development (GD14-GD15), further suggesting that it may play an important role in the development of the anorectum. However, the expression levels of BMP7 in ARM rats at the same stage were significantly lower, implying that downregulation of BMP7 expression during this essential stage of anorectal development may reduce the signals from endoderm to mesoderm and affect the transition from endoderm to intestinal epithelium, thus contributing to ARM. BMP7 expression gradually decreased in normal embryos after anal opening on GD16, suggesting that it may play an essential role during the initial morphogenesis of the anorectum but be less important during subsequent development. BMP7 expression thus demonstrated time-dependent changes during anorectal development.

Despite the likely complex multifactorial etiology, ARM is generally thought to arise through maldevelopment of the URS and a failure of fusion with the CM. The observations of anorectal development in our study were consistent with previous results [12, 15]. BMP7 expression in the anorectum showed different spatial distributions in normal and ARM embryos: from GD13 to GD15, BMP7-immunopositive cells were extensively detected in the key region during the progress of URS fusion with the CM, compared with only sporadic BMP7 immunostaining in this region in ARM embryos. These results suggest that morphogenic events in the anorectum depend on BMP7 signal transduction, and aberrant BMP7 expression may be responsible for abnormal anorectal morphogenesis.

ETU is known to disturb the expression of the shh signaling pathway during the development of the hindgut [13]. In addition, disruption of epithelial hedgehog signaling results in alterations in BMP signaling in the surrounding mesenchyme [14]. We therefore infer that misexpression of shh reduces signaling from the endoderm to the mesoderm and affects the expression of its targets, including BMP7. BMP7 levels were reduced in ETU-exposed embryos during hindgut development. This downregulation of BMP7 may provide a molecular explanation for the incomplete division of the cloaca which results in a variety of hindgut malformations.

In summary, we present new evidence for disrupted spatiotemporal expression of BMP7 during anorectal development in ARM embryos. The results suggest that BMP7 may play an important role in anorectal morphogenesis, and that decreased BMP7 expression might be related to the development of ARM. The detailed patterns of BMP7 expression established in this report provide a framework for understanding the role of BMP7 in hindgut development in both normal and ARM embryos. Further studies are needed to define the individual and interactive roles of BMP7 during development, and thus improve our understanding of the pathogenesis of ARM.

Acknowledgements

This study was supported by the National Natural Science Foundation of China (grant no. 81170578) and supported by the Outstanding Scientific Fund of Shengjing Hospital (grant no. m850).

Disclosure of conflict of interest

None.

Address correspondence to: Dr. Yu-Zuo Bai, Department of Pediatric Surgery, Shengjing Hospital, China Medical University, 36 Sanhao Street, Heping District, Shenyang 110004, P. R. China. Tel: 0086-24-9661557111; Fax: 0086-24-23892617; E-mail: baiyz@sj-hospital.org

References

[1] Van der Putte SC. Normal and abnormal development of the anorectum. J Pediatr Surg 1986; 21: 434-440.

[2] Peña A, Hong A. Advances in the management of anorectal malformations. Am J Surg 2000; 180: 370-376.

[3] Peña A, Guardino K, Tovilla JM, Levitt MA, Rodriguez G, Torres R. Bowel management for fecal incontinence in patients with anorectal malformations. J Pediatr Surg 1998; 33: 133-137.

[4] Bai Y, Yuan Z, Wang W, Zhao Y, Wang H, Wang W. Quality of life for children with fecal incontinence after surgically corrected anorectal malformation. J Pediatr Surg 2000; 35: 462-464.

[5] Levitt MA, Peña A. Outcomes from the correction of anorectal malformations. Curr Opin Pediatr 2005; 17: 394-401.

[6] Zhang T, Bai YZ, Wang da J, Jia HM, Yuan ZW, Wang WL. Spatiotemporal pattern analysis of transcription factor 4 in the developing anorectum of the rat embryo with anorectal malformations. Int J Colorectal Dis 2009; 24: 1039-1047.

[7] Dale L and Jones CM. BMP signaling in early Xenopus development. BioEssays 1999; 21: 751-760.

[8] Hammerschmidt M and Mullins MC. Dorsoventral patterning in the zebrafish: bone morphogenetic proteins and beyond. Results Probl Cell Differ 2002; 40: 72-95.

[9] Kishigami S and Mishina Y. BMP signaling and early embryonic patterning. Cytokine Growth Factor Rev 2005; 16: 265-278.

[10] Xu K, Wu X, Shapiro E, Huang H, Zhang L, Hickling D, Deng Y, Lee P, Li J, Lepor H, Grishina I. Bmp7 functions via a polarity mechanism to promote cloacal septation. PLoS One 2012; 7: e29372.

[11] Wu X, Ferrara C, Shapiro E, Grishina I. Bmp7 expression and null phenotype in the urogenital system suggest a role in re-organization of the urethral epithelium. Gene Expr Patterns 2009; 9: 224-230.

[12] Bai YZ, Chen H, Yuan ZW, Wang W. Normal and abnormal embryonic development of the anorectum in rats. J Pediatr Surg 2004; 39: 587-590.

[13] Mandhan P, Quan QB, Beasley S, Sullivan M. Sonic hedgehog, BMP4,and Hox genes in the development of anorectal malformations in ethylenethiourea-exposed fetal rats. J Pediatr Surg 2006; 41: 2041-2045.

[14] Runck LA, Method A, Bischoff A, Levitt M, Peña A, Collins MH, Gupta A, Shanmukhappa S, Wells JM, Guasch G. Defining the molecular pathologies in cloaca malformation: similarities between mouse and human. Dis Model Mech 2014; 7: 483-93.

[15] Boon MR, van der Horst G, van der Pluijm G, Tamsma JT, Smit JW, Rensen PC. Bone morphogenetic protein 7: a broad-spectrum growth factor with multiple target therapeutic potency. Cytokine Growth Factor Rev 2011; 22: 221-229.

[16] Qi BQ, Beasley SW, Frizelle FA. Clarification of the processes that lead to anorectal malformations in the ETU-induced rat model of imperforate anus. J Pediatr Surg 2002; 37: 1305-1312.

[17] Zhang T, Bai YZ, Zhang D, Zhang SW, Wang da J, Jia HM, Yuan ZW, Wang WL. Temporal and spatial expression of caudal-type homeobox gene-1 in the development of anorectal malformations in rat embryos. J Pediatr Surg 2009; 44: 1568-1574.